



OPEN ACCESS

EDITED BY
Dan Benjamini,
National Institute on Aging (NIH),
United States

REVIEWED BY
Kulam Najmudeen Magdoom,
Eunice Kennedy Shriver National
Institute of Child Health and Human
Development (NIH), United States
Katharina Schregel,
Heidelberg University Hospital,
Germany

*CORRESPONDENCE
Gwenaël Pagé,
gwenael.page@inserm.fr

SPECIALTY SECTION
This article was submitted to Medical
Physics and Imaging,
a section of the journal
Frontiers in Physics

RECEIVED 31 March 2022
ACCEPTED 02 August 2022
PUBLISHED 31 August 2022

CITATION
Pagé G, Garteiser P and Van Beers BE
(2022), Magnetic resonance
elastography of malignant tumors.
Front. Phys. 10:910036.
doi: 10.3389/fphy.2022.910036

COPYRIGHT
© 2022 Pagé, Garteiser and Van Beers.
This is an open-access article
distributed under the terms of the
[Creative Commons Attribution License
\(CC BY\)](https://creativecommons.org/licenses/by/4.0/). The use, distribution or
reproduction in other forums is
permitted, provided the original
author(s) and the copyright owner(s) are
credited and that the original
publication in this journal is cited, in
accordance with accepted academic
practice. No use, distribution or
reproduction is permitted which does
not comply with these terms.

Magnetic resonance elastography of malignant tumors

Gwenaël Pagé^{1*}, Philippe Garteiser¹ and Bernard E. Van Beers^{1,2}

¹Laboratory of Imaging Biomarkers, Center of Research on Inflammation, Université Paris Cité, Inserm, Paris, France, ²Department of Radiology, Beaujon University Hospital Paris Nord, AP-HP, Cllichy, France

Cancer biomechanical properties, including high stiffness, solid stress, and interstitial pressure, as well as altered micro-architecture, are drivers of tumorigenesis, invasiveness and resistance to treatment. Magnetic resonance elastography is an emergent non-invasive imaging method to assess the tumor mechanical properties in a spatially resolved fashion. Several MRE acquisition and reconstruction methods have been developed to assess tumors and surrounding tissues. It is increasingly recognized that the visco-elastic properties assessed with MRE are useful for characterizing malignant tumors and evaluating treatment response in various organs. Generally, malignant tumors, except brain tumors, have high stiffness and high visco-elastic ratio or fluidity. MRE transducers, acquisition sequences and reconstruction algorithms are continuously improved to increase depth penetration and spatial resolution, and limit artifacts at spatial discontinuities. Moreover, assessment of compression stiffening might provide new biomarkers of the altered physical traits of cancer. Increasing research and clinical validation will improve the efficacy of MRE for cancer characterization.

KEYWORDS

magnetic resonance elastography, cancer imaging, biomechanical properties, malignant tumor, biomarker

1 Introduction

Malignant tumors have four physical hallmarks which are high stiffness, solid stress, and interstitial fluid pressure, as well as altered micro-architecture. These biomechanical properties facilitate tumor progression and limit treatment efficacy by hindering drug delivery [1]. Magnetic resonance elastography (MRE) is increasingly used to assess tumor visco-elasticity [2–5]. This assessment may be useful for characterization of cancer severity and evaluation of treatment response [6–8].

2 MRE for tumor assessment

For reconstructing the tissue mechanical properties, MRE can be decomposed in three steps [9, 10]. First, an actuator is placed close to the tumor to generate mechanical vibrations. Second, a phase contrast MRI acquisition sequence, centred

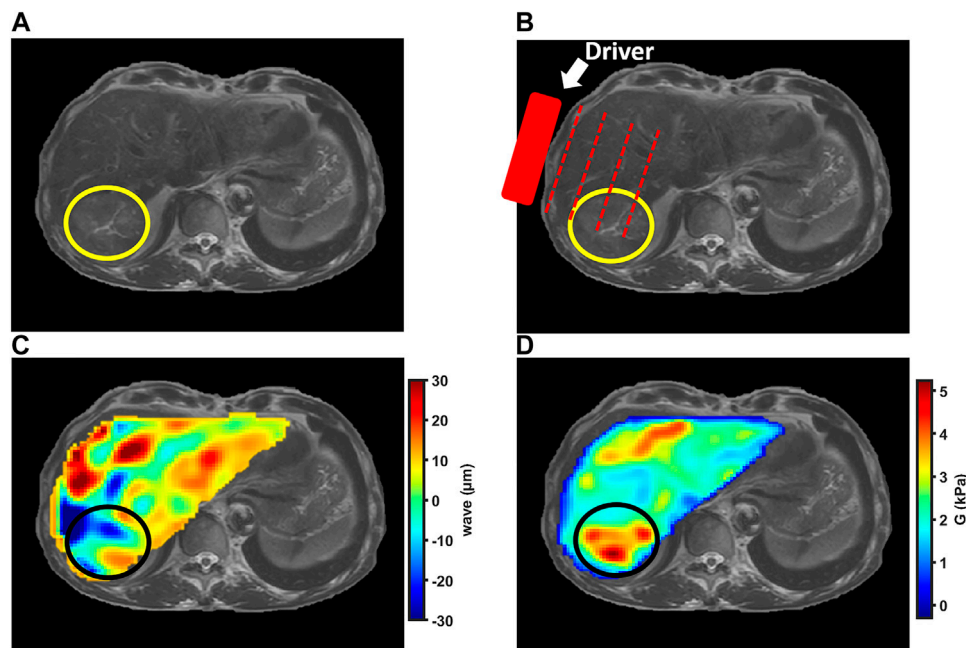


FIGURE 1

MRE examination in patient with hepatocellular carcinoma indicated by the circle. **(A)** Anatomic T2-weighted MR image of liver showing slightly hyperintense hepatocellular carcinoma in right liver lobe. **(B)** Anatomic MR image illustrating external driver position. **(C)** Shear wave color map showing propagating waves within the liver and tumor. **(D)** Shear modulus color map showing liver and hepatocellular carcinoma stiffness.

on the tumor, is used to encode the motion. Third, a reconstruction algorithm is used to assess the mechanical properties from shear wave propagation (Figure 1).

2.1 Actuators

Several types of actuators have been developed to propagate shear waves in tissues and tumors. The shape, size and power of the actuators are adapted to the explored organ. Moreover, drivers have been specifically developed to assess small animals in which tumors can be induced or implanted for preclinical studies.

2.1.1 Clinical studies

In early MRE studies, electromagnetic actuators have been used [11]. The drivers are composed of a coil connected to a piston. Using the B_0 of the MR scanner, an alternating current in the coil generates mechanical vibrations of the piston. This kind of actuator has been used to detect tumors located in breasts [11], to assess the mechanical properties of liver tumors [2] and to compare MRE results with histologic features in prostate cancer [12]. However, using this system, near field artefacts may occur with echo planar imaging [13].

Alternatively, pneumatic drivers which use air pressure waves to obtain mechanical vibrations, have been proposed. A speaker system generates sinusoidal displacements in a passive driver placed against the explored organ. System simplicity and easy configuration of frequency and wave amplitude are advantages of pneumatic drivers. Furthermore, the geometry of the membrane can be optimized for the explored organ, such as a pillow-like driver for propagating shear waves inside the brain. Pneumatic drivers have been used to explore various tumors in the brain [14, 15] and the liver [16]. They are easily positioned but they work mainly at a frequency below 100 Hz and have low frequency accuracy because of the relation with the resonant eigenmodes of the pneumatic pipes [17]. A specific transducer has been designed for tomoelastography [18]. It is composed of air driven pressure pads, one or two pads being placed on the anterior side and two pads on the posterior side [19, 20]. The multiple excitation sources allow for exploring retroperitoneal located organs such as the pancreas [20].

A mechanical actuator using a rotational eccentric mass to generate shear waves has also been developed. It is designed to easily be placed close to different organs such as the brain [21]. One disadvantage of the system is the coupling between frequency and amplitude of the shear waves. Hence, the actuator may be less tolerated at high frequency by sensitive patients.

2.1.2 Preclinical studies

In preclinical high field (7T) MRE scanners, external actuation is induced with piezoelectric transducers, electromechanical uniaxial shakers or loudspeakers. The last two systems need to be placed outside the bore. Shear waves are propagated to the tumors with a rigid carbon rod. Small animal studies have shown the ability to assess tumors implanted subcutaneously [22] or orthotopically in brain [23, 24], breast, pancreas [5] and colon [6]. Prostate tumors have also been examined ex-vivo [25]. Pepin et al. [26] used an electromechanical driver connected to a silver needle inserted in mice Hodgkin's lymphoma.

2.2 Motion encoding

In MRE, oscillating magnetic field gradients, also called motion-encoding gradients (MEGs), are used to encode the harmonic displacement in phase contrast images. The MEGs can have various shapes. Rectangular and trapezoidal MEGs have generally higher encoding efficiency than sinusoidal gradients. MEGs are typically inserted at each side of the refocusing pulse. One or more directions can be encoded, and for complete wave field characterization, encoding of the three spatial directions is needed.

The MEGs are inserted in several types of imaging sequences, including gradient-echo, spin-echo or echo-planar imaging. Echo-planar imaging reduces the acquisition time [27]. However, this kind of readout is associated with distortion artifacts which may have an impact on the displacement estimation. Moreover, echo-planar imaging is characterized by long echo times caused by the long echo train. At long echo times, the image signal may be drastically decreased, especially in tissues with short T2, such as the liver. In clinical practice, gradient-echo and echo-planar imaging are mainly used [28, 29].

MRE provides an image of the harmonic wave displacement at a particular time point of the oscillation. Since the motion is synchronized with the pulse sequence, several time points of the displacement are imaged by delaying the MEG. Typically, four to eight-time steps are acquired along a period of the oscillating displacement. Fourier transformation is applied to extract the fundamental harmonic component of the displacement field.

2.3 Mechanical properties assessment

Several reconstruction methods have been developed to assess the mechanical properties with MRE. The methods vary according to unwrapping algorithm, noise reduction, compression wave removal, and inversion algorithm.

2.3.1 Local frequency estimation

With the local frequency estimation the frequency of the wave displacement is assessed locally [30, 31]. The shear modulus G (Pa) is deduced from its equation into a local homogeneous, linear, isotropic and elastic solid

$$G = \rho \left(\frac{\omega}{\nu} \right)^2,$$

where ρ is the material density (typically assumed to be 1,000 kg/m³), ω the angular frequency of the mechanical excitation (rad/s) and ν the shear wave spatial frequency (m⁻¹). The local frequency estimation method assumes homogeneity and no attenuation, thus only the real part of the complex stiffness is provided. The method has been used in patients to assess breast [32, 33], liver [34] and prostate cancer stiffness [35]. It has also been extended to estimate tissue viscosity by applying the local frequency estimation on the curl of the displacement field [36].

2.3.2 Direct inversion

The complex shear modulus (G^*) can be expressed by direct inversion of the Helmholtz wave equation,

$$G^*(r, \omega) = -\rho\omega^2 \frac{u_i(r, \omega)}{u_{i,11}(r, \omega) + u_{i,22}(r, \omega) + u_{i,33}(r, \omega)}$$

where r is the spatial coordinate system (1, 2, 3), u the complex harmonic shear wave displacement, ω the angular frequency of the mechanical excitation and i , the motion-encoding direction [37, 38]. Direct inversion is performed after application of a high-pass filter to remove the longitudinal wave [39] and assuming that the viscoelastic medium is linear, isotropic and homogeneous.

Another common method to remove the compression waves is to apply a discrete curl operator to the displacement field before the inversion [40]. In contrast to high-pass filtering, the curl is applied in the three-dimensional space and requires wave displacement encoding along the three spatial directions.

As the shear modulus is a complex quantity, it can be expressed as $G^* = G' + iG''$. The real part G' and the imaginary part G'' correspond respectively to the storage modulus representing tissue elasticity and to the loss modulus representing tissue viscosity [41, 42]. Other parameters that represent the visco-elastic ratio can be derived, including the damping ratio ($\zeta = \frac{G''}{2G'}$) and the shear modulus phase angle ($\varphi = \arctan(\frac{G''}{G'})$) which is also called fluidity, ranging from 0° for purely elastic materials to 90° for purely viscous materials [10, 43].

Direct inversion has been used in the clinics to assess the viscoelastic properties of breast [11, 44], liver [2] and prostate [25] tumors. It has also been used in preclinical MRE to assess subcutaneous [22] and orthotopic tumors [23].

2.3.3 Multifrequency direct inversion

With multifrequency direct inversion, multiple wave data sets acquired at different vibrational frequencies are combined [45]. With a variant of the method, called multifrequency dual viscoelastic reconstruction, frequency averaging is performed during the computation of the magnitude and the phase of the complex shear modulus rather than averaging the complex shear moduli obtained at each frequency [46].

More recently, tomoelastography has been introduced. It consists in using spatial filters in *k*-space to obtain shear waves in multiple directions. The shear wave speed and the attenuation are then averaged over all directions and frequencies. This method when used with multiple drivers placed around the explored area [19] is particularly promising to assess tumors located inside deep organs such as the pancreas. By increasing data quantity, multifrequency direct inversion increases the stability and the reliability of MRE. However, scan time can be long. Tomoelastography has already been used in the clinics to explore brain, liver, pancreas and prostate cancers [7, 20, 47, 48]. With the multifrequency direct inversion methods, the frequency dependence of the shear modulus is not considered.

2.3.4 Finite element method

The local frequency estimation and direct inversion assume local homogeneity. These methods work well in areas where the elasticity is almost constant. However, it has been reported that the homogeneity assumption may cause errors in regions where the elasticity variation is high [49].

There are finite element methods in which the local homogeneity assumption is not used. These methods are categorized into two groups: direct [50] and iterative methods [51, 52]. In the direct methods, the discretized equation of motion is rearranged to result in a system of equations with the shear modulus parameters as unknowns, which can be solved directly for a map of the shear modulus. Alternatively, for iterative methods, the inverse problem is considered as an optimization problem in which the shear modulus is changed iteratively to minimize the error between measured displacement and the simulated displacements [53]. The finite element method has been used to measure the mechanical properties of prostate cancer [12].

2.4 Comparisons of MRE methods

As described in this section, various MRE methods have been developed to reconstruct the tissue mechanical properties. Different mechanical actuators, MR imaging sequences, and reconstruction algorithms are used. How these various parameters influence the results of mechanical properties measurements is a topic of ongoing investigation. In chronic liver disease, Huwart et al. prospectively compared the performance of MRE using echo-planar and spin-echo

imaging for staging of hepatic fibrosis [27]. They showed that echo-planar imaging substantially decreased the data acquisition time, while maintaining the image quality and diagnostic performance for staging liver fibrosis.

More recently, the diagnostic performance of 2D gradient-echo and 3D echo-planar MRE has been compared to stage liver fibrosis. It was observed that the technical failure rate was lower with 3D echo-planar versus 2D gradient-echo MRE, but the diagnostic performance of both MRE sequences was similar when the same shear wave frequency was used [29, 54, 55]. The two MRE acquisitions differed regarding image acquisition (2D versus 3D, gradient-echo versus echo-planar), slice thickness, and reconstruction algorithm.

Moreover, lower stiffness values were observed with 3D echo-planar MRE than with 2D gradient-echo or 2D echo-planar MRE. This has been attributed to the fact that the 2D algorithm assumes all waves propagate in the imaging plane, which can lead to overestimation of the wavelengths of waves intersecting the imaging plane obliquely [55].

When comparing 2D echo-planar and gradient-echo MRE in the liver, the image quality scores were significantly higher and the failure rate substantially lower when using echo-planar imaging [56]. The higher quality with echo-planar MRE may be explained by the fact that the sequence is less sensitive to T2* decay than gradient-echo imaging and because its acquisition time is shorter, allowing single breath-hold acquisitions in the liver.

In the normal brain, it has been found that stiffness values obtained with a finite element model approach were 40% higher than those obtained with direct inversion using a curl method [57]. These higher values may be explained by lower noise sensitivity with a finite element model [58].

As the measured stiffness depends on the choice of data acquisition and image reconstruction, it has been recommended to normalize stiffness measurements to a reference tissue. In brain cancer patients, tissue stiffness has been measured relative to healthy white matter [14]. In a cohort of patients with solid pancreatic masses, it has been shown that the stiffness ratio (calculated as the ratio of mass stiffness to the parenchymal stiffness) outperformed stiffness for differentiating between pancreatic ductal adenocarcinomas and benign mass forming pancreatitis [59]. However, using a reference tissue for tumor MRE may be limited by the variations of reference stiffness related to age or disease (such as liver fibrosis in patients with liver cancer).

Various shear wave frequencies are used for MRE. In clinical studies, frequencies below 200 Hz (usually between 40 and 60 Hz) are used. In small animal studies, higher frequencies between 100 and 1,000 Hz are often used. Increasing the frequency improves the spatial resolution but decreases shear wave penetration. For the clinical MRE assessment of the deep-seated pancreas, it has been observed that more consistent results were obtained at 40 Hz than at 60 Hz [28].

Increasing the frequency increases the apparent stiffness [60]. This shear wave frequency dispersion may complicate comparisons between MRE studies performed at different frequencies. However, when probed with multifrequency MRE, the frequency dispersion coefficient may give additional information about tissue structure [61–63]. The potential value of multifrequency MRE in cancer remains to be determined.

One should also be aware of shear wave frequency differences when comparing stiffness results between MRE and ultrasound elastography. Indeed, whereas transient ultrasound elastography uses 50 Hz, acoustic radiation force impulse-based techniques have most of their energy between 120 and 160 Hz [64, 65]. Moreover, there are other differences between MRE and ultrasound elastography. First, ultrasound work is based on transient excitation and usually measures wave speed, but this is a group velocity rather than a phase velocity. Second, Young's modulus (compression modulus) is usually the quantity reported at ultrasound elastography, which is typically three-times the shear modulus that is reported with MRE [10].

3 Biophysical properties of cancer and elastography studies in animals

During the recent decades, our understanding of cancer has evolved, and malignant tumors are currently viewed as aberrant organs composed of tumor cells and their surrounding stroma, both of which influence the biomechanical properties of cancer [66–68]. These biomechanical properties include high stiffness, solid stress and interstitial fluid pressure. These abnormal physical traits affect tumor progression and treatment resistance [69, 70].

3.1 Tumor biomechanical components

3.1.1 Definitions and origins of high stiffness, solid stress and fluid pressure.

3.1.1.1 Stiffness

Stiffness or rigidity is an intrinsic property of tissue defined as the resistance of the tissue to the applied force. Stiffness is mainly determined by extracellular matrix composition and organization [71]. Particularly, tumor stiffness is related to collagen deposition and cross-linking [5]. It has been shown that hyaluronic acid swelling also increases tumor stiffness [72].

Moreover, tumor stiffness is influenced by extracellular matrix modifications caused by stromal cells. Indeed, it has been shown that the fraction of stroma cells and the activity of fibroblasts and immune cells correlate with stiffness [23, 73, 74]. In contrast, necrotic areas tend to decrease tumor stiffness [75].

In addition to the structural part of tissue stiffness related to matrix deposition, a functional part related to soft tissue water

content has been identified [60]. Indeed, several studies have reported elevated stiffness in tissues with inflammation and high interstitial or intravascular pressure [63, 76, 77].

3.1.1.2 Solid stress

The solid stress is a mechanical force influenced by the solid components of the tumor, including the cancer cells, the collagen fibers and the hyaluronan acid gel [68]. Cellular proliferation, matrix deposition, cell contraction, and abnormal growth patterns all lead to compressive and tensile solid stresses within tumors (1). Solid stress can thus be generated by both extracellular matrix and cells, in contrast to tumor stiffness which is mainly a property of the extracellular matrix [78, 79]. This difference between solid stress and stiffness is illustrated by the fact that primary and metastatic tumors can have substantially different levels of solid stress despite similar stiffness values [78].

3.1.1.3 Interstitial fluid pressure

The isotropic fluid pressure includes the pressure exerted by liquid within the interstitial space, blood and lymphatic vessels. In tumors, elevated interstitial fluid pressure is caused by leakage of plasma from abnormally permeable tumor blood vessels and insufficient lymphatic drainage. It adds to the solid stress to compose the total tumor pressure, which is dominated by the solid stress component, at least in pancreatic tumors [80].

3.2.1 Effects of abnormal physical traits on tumor progression.

High tumor stiffness, solid stress and interstitial fluid pressure promote tumor progression and resistance to treatment through activation of a large cascade of mechanoresponsive pathways in cancer cells and stromal cells, including endothelial, epithelial, mesenchymal and immune cells [1, 81, 82]. The mechanotransduction effect of high solid stress has been exemplified in a recent study showing that the application on the healthy mouse colon of an external pressure similar in magnitude to the stress induced by tumor growth, caused the stimulation of tumorigenic pathways without changes in tissue stiffness [83].

It should be noted that the physical traits favouring tumor progression are intricate. Physicists were tempted to consider the steps of the cancer metastasis cascade as single events caused by one mechanical alteration. However, this simple view has been challenged by the finding that several cancer parameters influence each other and contribute to tumor growth and cancer progression [84]. Indeed, by compressing blood and lymphatic vessels, solid stresses contribute to increased fluid pressure in tumors. Through strain-stiffening, solid stresses also increase tumor stiffness. Finally, fluid flow activates fibroblasts, which then contribute to increased solid stresses and stiffness values [1].

Globally, the changing biophysical properties in cancer are strongly coupled with abnormalities in the tumor vasculature and

extravascular compartments [79]. Indeed, high solid stresses related to high matrix stiffness and hyper-proliferative pressure in tumors are large enough to compress the blood and lymphatic vessels, impairing blood flow and the delivery of oxygen, drugs, and immune cells [85–87]. Impaired drug delivery is also promoted by the high interstitial fluid pressure secondary to the hyperpermeability of tumor angiogenic vessels [88]. Moreover, the pressure difference in the periphery of the tumor causes fluid leaking from the vessels at the tumor boundaries in the surrounding tissue. This facilitates the transport of cancer cells into the host tissue, increasing tumor progression and metastatic risk [89].

Both dysregulated angiogenesis which produces leaky blood vessels and desmoplasia which compresses the vessels, reduce the capacity of blood vessels to deliver oxygen to tumors. Hypoxia not only promotes disease progression and resistance to radiation and some chemotherapies, but also causes immunosuppression in the tumor microenvironment. Moreover, newly formed immature blood vessels cannot distribute infiltrating immune cells efficiently, whereas excessive fibrosis poses a physical barrier to immune cell migration in the tumor. Accordingly, hypoxia is associated with poor survival and resistance to treatment, especially to newly developed immunotherapies [90].

Improving drug delivery can be achieved by repairing the hyperpermeability of tumor blood vessels and/or decompressing tumor blood vessels by targeting tumor stromal components [79]. Restoration of the vascular function can be achieved with vascular normalization strategies, whereas decompression of tumor vessels can be obtained with stress-alleviating methods that target the tumor extracellular matrix and/or cancer associated fibroblasts. Most antiangiogenic agents target the vascular endothelial growth factor or its receptors. Recently, it was shown that metronomic chemotherapy and immunotherapy also can induce vascular normalization [90–92].

In contrast, stress alleviation strategies can be obtained with matrix-depleting agents, such as collagenase, relaxin, and matrix metalloproteinases. These agents have been used to reduce collagen or hyaluronic acid levels in tumors and have been shown to improve the efficacy of anticancer drugs in animal models [5, 93, 94]. Furthermore, the PEGylated human recombinant hyaluronidase (PEGPH20) has been used to reduce fibrosis and solid stress and increase survival in mouse models [95].

A second type of matrix normalization involves reversing vessel compression with cancer associated fibroblast reprogramming therapies. Hereby, cancer associated fibroblasts are turned quiescent such that they produce a smaller magnitude of forces. One such drug is losartan, which is an anti-hypertensive drug with decades of use in patients with high blood pressure. In preclinical models of pancreatic adenocarcinoma, losartan was used to decrease solid stress and decompress blood vessel, improving chemotherapy efficacy [96]. However, results in clinical trials are not yet

convincing. More precisely, if losartan has shown some promising clinical results in a phase II clinical trial [97], it is not the case for PEGPH20 [97, 98]. There are several reasons for this, including toxicity, complexity and heterogeneity of tumor microenvironment.

Indeed, matrix alleviating therapies may have contra-intuitive results. Whereas *in vivo* and *in vitro* studies have shown that extracellular matrix stiffness promotes breast, pancreas and brain cancer progression [99–102], it has recently been observed that fibrosis may have a dual role in tumor invasion as it produces stiffness induced mechano-signals for tumor progression but also mechanically restrains tumor spread [103]. The discordant results about the promoter versus protective role of fibrosis may at least be partially explained by tumor heterogeneity [5]. Indeed, heterogeneity poses the risk of obtaining inconsistent results. Moreover, the heterogeneous nature of pancreatic adenocarcinoma tissue has been reported to be a driver of aggression. Indeed, the periductal region surrounding tumor glands has been found to have increased stiffness which drives metastasis [92]. These findings suggest that the architecture and mechanics of collagen fibers adjacent to the epithelial lesion, and not bulk collagen abundance, may be an indicator of pancreatic adenocarcinoma aggression.

3.2.2 Measurement methods of cancer biophysical properties

Classically, tissue stiffness and viscoelasticity are measured *ex-vivo* with invasive methods, including atomic force microscopy and rheometry [104]. Currently, *in vivo* measurements of stiffness and viscoelasticity can be performed with ultrasound and MR elastography [105].

The measurement of solid stress remains more difficult, even with invasive methods. Stylianopoulos et al. [106] proposed to cut excised tumors and to measure the stress relaxation as the extent of tumor opening normalized to the diameter of the tumor. By using mathematical modelling, the growth-induced stress could be assessed [106, 107]. The method has been extended by Nia et al. [78] to quantify the deformation of the tumor cut plane with ultrasonography.

In vivo, the total tumor pressure, solid stress and interstitial fluid pressure can be quantified separately by inserting a piezoelectric pressure catheter inside the tumor [80, 95]. This invasive method is not routinely used in humans.

Non-invasive methods to assess tumor solid stress are being developed, using ultrasound or MR elastography measurements. Islam et al. have proposed a poroelastography model to quantify solid stress with ultrasound elastography [108, 109]. Fovargue et al. have suggested to investigate the mechanical properties of the tissue surrounding the tumor to estimate its pressure with MRE [110]. Based on the compression stiffening effect [111, 112], Pagé et al. have shown the potential of compression MRE to assess tumor solid stress in liver cancer [113, 114].

Non-invasive elastography may also be useful to assess fluid pressure by showing a correlation between fluid pressure and viscoelasticity. At ultrasound elastography, Rotemberg et al. and Gennisson et al. showed a relation between fluid pressure and tissue stiffness (measured with shear wave speed) in liver and kidney [115, 116]. Rotemberg et al. demonstrated a correlation between shear wave speed and portal venous pressure in excised canine liver. Gennisson et al. observed high kidney shear wave speed after renal vein or ureter ligation and low speed after renal artery ligation in pigs. With MRE, a correlation between liver and spleen viscoelasticity and portal venous pressure in small animals and in patients has been reported [77, 117–119].

Alternatively to elastography, dynamic-contrast enhanced MR imaging has been proposed to assess fluid flow and interstitial pressure in tumors [120, 121].

3.2.3 Non-invasive preclinical investigations with elastography

Elastography measurements have been performed in tumors implanted in mice to investigate the relation between stiffness and tumor progression [8, 73, 122]. In soft brain tumors (glioblastomas) Schregel et al. [8] observed decreased stiffness with tumor progression using MRE. In contrast, Ahmed et al. [122] found a stiffness increase during progression of liver metastases from pancreatic adenocarcinomas using shear wave elastography. In an ultrasound elastography study, Riegler et al. [73] observed a strong correlation between stiffness and tumor volume for slow growing tumors such as breast and pancreatic cancers.

Moreover, MRE studies have shown stiffness decrease with collagenase in breast cancer [5], anti-VEGF antibodies in glioblastoma [8], vascular disrupting agents in colon tumor and colorectal cancer [6, 22] and chemotherapeutic agents in glioma [26]. Several causes have been mentioned for this decreased stiffness. It has been related to the direct effect of collagenase on fibrosis, to the vascular normalization by anti-VEGF antibodies, and to the association between vascular disrupting agent effect and tumor necrosis. For the stiffness decrease with a chemotherapy treatment, it has been postulated that changes in interstitial pressures, cellularity, and extracellular components are involved [27]. However, the actual mechanism of the stiffness change is unknown.

The effect of radiation therapy was investigated on glioblastomas orthotopically implanted in mice [24]. In this study, the authors observed a decrease of tumor stiffness over time independently of radiation therapy.

In another study, the effect of radiation therapy was assessed in pancreatic cancer implanted in mice [123]. Here, a decrease of shear modulus was observed in pancreatic tumors after stereotactic body radiation therapy. It was concluded that shear modulus could help to differentiate between tumors responsive to radiation therapy and non-responsive tumors.

At ultrasound elastography, it has been observed that the tissue stiffness correlated with drug delivery in two orthotopic mouse models of pancreatic tumors [124]. However, as already discussed, drug delivery depends not only tumor stiffness, but also on solid and fluid pressure and on tumor heterogeneity [111].

It is expected that non-invasive measurements of solid stress with compression MRE may result in new elastography modalities to decouple stiffness from solid stress and improve our understanding of the roles of stiffness and stress in tumor progression and treatment response [111, 114]. Finally, high resolution ultrasound and MR elastography may be used to explore cancer heterogeneity [5, 125].

3.4. MRE for tumor assessment in patients

3.4.1 Liver

MRE is used to assess the biomechanical properties not only of hepatic tumors, but also of the liver parenchyma. Indeed, MRE offers good diagnostic accuracy to assess the features of chronic liver disease, including fibrosis, cirrhosis, and portal hypertension [118, 126–133]. These factors, especially liver cirrhosis, are promoters of hepatocellular carcinoma development [134].

3.4.1.1. Investigating the risk of cancer development

In a retrospective MRE study, the liver stiffness was measured in 301 patients with chronic liver disease of which 66 patients had hepatocellular carcinomas [135]. It was found that the patients with hepatocellular carcinomas had higher liver stiffness (mean: 5.0 kPa) than those without it (3.8 kPa). Moreover, at multivariate analysis, liver stiffness was the only significant predictor of hepatocellular carcinoma, in contrast to age, gender and blood markers.

In another study, two MRE acquisitions were performed at 12-months interval in 161 patients with chronic liver diseases [136]. The patients were divided into three groups according to sequential changes in liver stiffness as follows: high (> 4.7 kPa) on the first MRE (group A), low (< 3 kPa) on both MRE examinations (group C) and other combinations (group B). Group A classification was an independent risk factor for hepatocellular carcinoma development. The authors concluded that patients with chronic liver disease and high liver stiffness on previous MRE examinations were at high risk for developing hepatocellular carcinoma.

3.4.1.2 Characterization of liver tumors

Diffusion-weighted and dynamic contrast-enhanced MRI are routinely performed for tumor detection and characterization [137]. By investigating the mechanical properties, MRE offers a new opportunity for tumor characterization. Venkatesh et al. [16] studied the stiffness of 44 liver tumors. They found that the

malignant tumors had significantly higher stiffness than the liver (10.1 ± 3.6 kPa versus 2.3 ± 0.3 kPa), whereas benign tumor stiffness (2.7 ± 0.4) was similar to the liver stiffness.

In another study, MRE and diffusion-weighted imaging were performed in 79 patients with 124 focal liver lesions [138]. Again, mean stiffness of malignant tumors was significantly higher than that of benign lesions (7.9 vs. 3.1 kPa, $p < 0.0001$) and MRE had higher diagnostic performance than diffusion-weighted imaging for differentiating between benign and malignant tumors (AUC = 0.99 versus AUC = 0.87; $p = 0.002$).

Visco-elastic properties of 72 liver tumors were assessed [2]. In contrast to the two previous studies, 3D images were acquired, allowing for the reconstruction of the complex shear modulus from the curl reconstruction method. It was observed that the increase of complex shear modulus magnitude in malignant tumors was mainly caused by an increase of the loss modulus (viscosity) rather than the storage modulus (elasticity). These results have been confirmed in a recent study showing high tumor stiffness and fluidity in malignant liver tumors [7].

3.4.1.3 Recurrence

Tumor recurrence complicates 70% of hepatocellular carcinomas after hepatic resection at 5 years and is the expression of both early intrahepatic metastases and late development of *de novo* tumors. Predictive factors for early recurrence within 24 months of surgery, are mainly tumor-related (i.e., tumor size, tumor number, presence of tumor budding, microsatellites and vascular invasion). In contrast, late recurrence (>24 months after surgery) is probably related to the evolution of the underlying chronic liver disease, including fibrosis stage and portal hypertension severity [139, 140].

This difference in the cause of early and late recurrence explains that tumor stiffness has been explored as predictive marker of early recurrence, whereas liver and spleen stiffness has been assessed as marker of late recurrence [139, 141, 142]. In a cohort of 99 patients, Wang et al. found that high tumor stiffness and vascular invasion were two determinants associated with early hepatocellular carcinoma recurrence after hepatectomy [141].

For predicting late tumor recurrence, Marasco et al. measured liver and spleen stiffness in 175 patients before surgical resection and showed that spleen stiffness was an independent predictor of late hepatocellular carcinoma recurrence. Similarly, in a study performed in 192 patients, Cho et al. [142] observed that liver stiffness before treatment was a predictor of late hepatocellular carcinoma recurrence.

3.4.1.4 Therapy response

Few studies have been performed to assess the evolution of hepatocellular carcinoma mechanical properties after treatment. Gordic et al. [143] quantified hepatocellular carcinoma stiffness in patients after transarterial chemoembolization or yttrium radioembolization. Decrease of the mechanical properties was

observed in the treated patients. This decrease was paralleled by an increase of tumor necrosis.

Qayyum et al. [144] observed an increase of the hepatocellular stiffness after 6-weeks immunotherapy with pembrolizumab in patients with hepatocellular carcinomas. The stiffness was correlated with tumor T lymphocytes infiltration, overall survival and time to progression.

3.4.2 Breast

Manual palpation is an easy procedure to detect breast lumps but it has limited sensitivity of about 55% to detect breast cancer [145]. MRI can be used to improve breast cancer diagnosis. Dynamic contrast-enhanced MRI is routinely performed in the clinics for breast tumor detection and characterization, and more recently it has been associated with diffusion weighted and T₂-weighted imaging to perform a multiparametric analysis [146]. However, contrast-enhanced MRI still has many false-positive results [147].

Breast MRE represents an additional tool for assessing breast cancer. Early studies showed the feasibility to assess the mechanical properties of breast cancer, including stiffness, visco-elasticity, phase angle, anisotropy and frequency dispersion [11, 33, 40, 41, 148–150]. Globally, these studies and more recent clinical series [44, 151] showed increased viscosity and phase angle in malignant tumors with variable changes in elasticity, which may be increased or decreased relative to that in benign lesions. This variability may at least be partially explained by the type of breast lesions that are included in the studies.

Assessment of breast cancer is already performed in the clinics with ultrasound elastography [152, 153]. The accessibility of the organ and the fact that ultrasound elastography is easy to use and widely available are arguments in favour of this method. However, MRE provides better spatial resolution and encodes the three spatial directions of the shear wave displacement improving the accuracy of mechanical parameter quantification. This could be relevant to investigate the relation between mechanical parameters and tumor heterogeneity [5].

3.4.3 Brain

Surgical strategies to treat intracranial tumors depend on tumor consistency. Soft tumors generally require less invasive surgery, while firm fibrotic tumors may require more open surgery. It has been shown that determining brain tumor stiffness with MRE is feasible and correlates with surgical consistency [3, 154–157]. Another important factor in determining the difficulty of resection is the adherence of the tumor to the surrounding tissue, where tumors that are adherent are more difficult to remove. To address this problem, slip interface imaging has been developed. The basic idea is that if two adjacent compartments of tissue are free to move independently of one another, then as a shear wave

propagates across the boundary, a discontinuity will be created. This discontinuity can be detected on a shear strain map [158].

Regarding tumor characterization, several studies have suggested that benign meningiomas are the stiffest intracranial tumors and that they have the highest fluidity (phase angle) and viscosity (loss modulus) [3, 159, 160]. In contrast, malignant tumors, especially glioblastomas, are characterized by low stiffness (soft tumors) and low fluidity and viscosity [43]. However, discrimination between different tumor types based on the values of the mechanical parameters is currently limited because of substantial overlap of the distributions of each of the parameters from different tumors. To remove the bias in the reported values of the mechanical parameters caused by differences of hardware, reconstruction methods and signal to noise ratios, it has been recommended to compute the difference in each shear modulus parameter between the tumor and the contralateral normal appearing white matter. This has resulted in some improvement in defining the distribution of values in different tumors. Particularly, the distribution of delta loss modulus values in meningiomas is unique in that it is the only distribution with a predominantly unipolar positive distribution. Nevertheless, even after normalizing a wide range of values for essentially all tumors and all parameters remains [3].

Further characterization of gliomas with MRE has been shown by Pepin et al. [161]. In their study, gliomas were softer than healthy brain parenchyma, with grade IV tumors softer than grade II. Tumors with an isocitrate dehydrogenase 1 (IDH1) gene mutation were significantly stiffer than those with wild type IDH1. The authors conclude that noninvasive determination of tumor grade and IDH1 mutation may result in improved stratification of patients for different treatment options and the evaluation of novel therapeutics.

The potential role of fluidity in brain tumor aggressiveness has been described by Streitberger et al. The authors found that fluidity of neurotumors is anomalous in that it decreases as water content increases, enabling glioblastomas to infiltratively finger in normal surrounding brain matter [43]. The quantification of the fluidity as marker of invasiveness in brain cancer could potentially improve clinical prognosis and therapeutic management of patients.

Most applications of brain MRE assumes an isotropic tissue while brain white matter is likely to produce an anisotropic mechanical response [162]. Not taking the anisotropy into consideration can lead to misestimation of mechanical parameters in the normal brain, but this is probably less relevant in brain cancer. To measure the anisotropic effect, several MRE reconstruction methods have been developed [163–165].

Before the adoption of brain tumor MRE in routine clinical practice, more studies should be performed and the

reproducibility MRE parameters as imaging biomarkers of cancer should be assessed. Further studies on the relation between tumor mechanical parameters and extracellular matrix composition should also be performed.

3.4.4 Prostate

Multiparametric MRI including T₂-weighted imaging and dynamic contrast-enhanced MRI has shown its usefulness in prostate cancer diagnosis. However, the specificity remains low and prostate biopsy is still required [166]. Evaluation of stiffness could provide additional information about prostate cancer characterization. Indeed, ex-vivo studies have shown the high effect of collagen deposition in the evaluation of prostate tumor grade [167, 168].

A challenge in prostate cancer MRE is to propagate shear waves inside the organ. Specific drivers have been developed to respond to this need [169, 170]. In 2011, Li et al. have provided an *in vivo* study evaluating the viscoelastic properties in 12 patients with prostate cancer and 14 with prostatitis [35]. A transducer was placed above the pubis to transmit mechanical waves at 100 Hz. Prostate cancer was found to have significantly higher stiffness than the healthy peripheral zone (6.55 ± 0.47 kPa vs. 2.26 ± 0.45 kPa, $p < 0.01$) and a positive correlation was observed between elasticity of prostate cancer and Gleason score. Moreover, viscoelastic properties provided a good separation between malignant and benign prostate tissue (elasticity: 6.55 ± 0.47 kPa vs. 1.99 ± 0.66 kPa, $p < 0.01$; viscosity: 6.56 ± 0.99 Pa s vs. 2.13 ± 0.21 Pa s, $p < 0.01$).

In a later study, Sahebjavaher et al. [12] used a transducer placed against the patient perineum. They have evaluated the repeatability in six volunteers and performed MRE acquisitions in 11 patients. Despite the poor repeatability results (25% variation in stiffness), a significant difference in stiffness was found between cancerous and normal tissue.

More recently, Dittmann et al. have shown the benefit of tomoelastography with drivers placed around the pelvis to assess prostate mechanical properties [19]. Twelve healthy volunteers and three subjects with a malignant prostate lesion were explored using three excitation frequencies (60 Hz, 70 and 80 Hz). Compared to the previous study, good reproducibility was found (3.7% and 2.7% in the peripheral and central prostate zone respectively). Consistent with the studies of Li and Sahebjavaher [12, 35] the shear waves speed in prostate cancer was higher than in healthy tissue.

In a recent prospective study with 208 participants, it was shown with tomoelastography that prostate cancer stiffness and fluidity were higher in prostate cancer than in benign prostatic disease. Multiparametric MRI combined with stiffness and fluidity measurements enabled detection of prostate cancer with 95% specificity, which was significantly higher than with use of multiparametric MRI alone (77%) [48].

3.4.5 Pancreas

Pancreatic ductal adenocarcinoma is a highly aggressive cancer, the overall 5-years survival rate among patients with pancreatic cancer being less than 5 % [91, 171]. It is characterized by a dense and rich stroma which plays a critical but debated role in its progression, as explained above [103]. The quantification of pancreatic cancer mechanical properties could help to evaluate its severity. However, the pancreas is a deep-lying organ and it is difficult to transmit mechanical shear waves in the pancreas of obese patients who are at risk of pancreatic ductal adenocarcinoma development [172].

Improvement in sequence acquisition time (use of echo planar imaging, parallel imaging) and development of new actuators (with tomoelastography) to propagate shear waves in deeply located organs, has increased the capacity of MRE to estimate the mechanical parameters of the pancreas [28, 173–175]. Several recent studies have shown the good diagnostic performance of MRE to differentiate between benign and malignant pancreatic masses [4, 20, 28, 172]. Pancreatic adenocarcinomas and malignant endocrine tumors exhibit higher stiffness and fluidity than the normal pancreas and benign lesions, including autoimmune pancreatitis.

3.4.6 Kidney

MRE is increasingly used to investigate the renal mechanical parameters. Preliminary studies have shown the feasibility of MRE to estimate the renal stiffness [176] and to assess the renal mechanical parameter variations caused by hydration and urinary status [177]. In a study published in 2018, the viscoelastic parameters of small renal tumors were assessed in 19 patients [178]. Compared to dynamic contrast-enhanced and diffusion-weighted imaging, MRE viscoelastic parameters provided the best discrimination between renal oncocytomas and carcinomas. In accordance with the literature in ultrasound elastography [179], malignant tumors were stiffer than benign lesions.

4 Discussion

MRE is an emerging method to assess cancer. Increasing number of preclinical and clinical studies show the potential of MRE for cancer characterization and treatment follow-up. When evaluating the surrounding tissue, the usefulness of MRE to predict the risk of cancer occurrence or recurrence has also been shown [139, 180].

Generally, malignant tumors, except brain tumors, have elevated stiffness and mainly elevated fluidity relative to the surrounding parenchyma and relative to benign tumors and pseudo-tumors. This is a general trend and there is some overlap of the biomechanical properties between benign and malignant tumors. In the brain, glioblastomas have variable stiffness and low fluidity enabling them to infiltratively finger in normal surrounding brain matter [43].

4.1 Issues of MRE technique in cancer investigation

MRE is still a recent method that is not yet standardized. Differences in generation of mechanical vibrations (frequency of the mechanical shear waves), in acquisition and reconstruction methods between studies may bias the mechanical parameter values. There is thus a clear need for method standardization, reproducibility assessment and multicenter clinical validation.

From a technical point of view, MRE is still limited for the examination of deep-lying tumors or brain tumors. Pancreas cancer imaging is difficult because the pancreas is retroperitoneal and the shear waves are attenuated by more superficial structures of the abdomen including adipose tissue, colon, stomach and liver. Therefore, the wave amplitude may not be sufficient to obtain accurate estimation of the pancreatic tumor stiffness. Specific transducers have been developed with multiple drivers placed around the abdomen to increase the number of sources providing mechanical vibrations [173].

Ongoing research is also performed with passive elastography [181]. The method uses shear waves generated naturally from cardiac motion or blood pulsatility. Passive elastography might be interesting to investigate cancers located in organs where shear waves cannot be transmitted with sufficient amplitude from an external driver, such as the brain.

Another limitation of cancer MRE is related to small tumor size. In some studies, patients with lesions smaller than 10 mm in the liver [16] or 20 mm in the brain [161] have been excluded. The assessment of early cancer may be limited, as small tumors cannot be distinguished from surrounding parenchyma because of large point-spread function [182]. MRE acquisition with echo planar imaging may reduce the scan time and increase the matrix resolution [183, 184].

Still another limitation is related to the homogeneity assumption often used for stiffness assessment. At the tissue-tumor interface especially, a large difference between the mechanical properties can affect the homogeneity assumption. A wave inversion method, called heterogeneous multifrequency direct inversion has been developed to accommodate heterogeneous elasticity within a direct inversion by incorporating first-order gradients and combining results from a narrow band of multiple frequencies [185].

4.2 Perspectives

MRE may be used to assess the altered physical traits in cancer, i.e., high stiffness, interstitial fluid pressure and solid stress, and altered micro-architecture. This non-invasive assessment may help understanding cancer dynamics and diagnosing cancer aggressiveness.

Tumor stiffness and visco-elasticity which are related to collagen density and cross-linking but also to fluid pressure are measured with basal MRE [5, 6, 77, 118]. However, compression MRE assessing non-linear stiffness (compression stiffening) may be useful to

evaluate tumor solid stress which is influenced by the solid elements of the tumor, including cells and extracellular matrix [114, 186, 187]. Assessing tumor solid stress with compression MRE might have prognostic significance, as it has been recently reported that microvascular invasion in patients with hepatocellular carcinoma can be assessed with compression MRE [188].

Tumor heterogeneity which also plays an important role in cancer severity might be further assessed with high resolution MRE, radiomics and deep learning [189].

Further studies should investigate the relation between MRE parameters, including multifrequency MRE and MRE under compression, and altered physical parameters as determinants of cancer aggressiveness.

In conclusion, MRE is an emergent method to quantify tumor mechanical properties, offering a clinically usable method for determining cancer prognosis and assessing treatment response. Increasing research and clinical validation will improve the efficacy of MRE for cancer characterization.

Author contributions

GP, PG, and BVB conceived the manuscript. GP and BVB wrote the manuscript. PG and BVB revised and edited the manuscript.

References

- Nia HT, Munn LL, Jain RK. Physical traits of cancer. *Science* (2020) 370:543.14–545. doi:10.1126/science.370.6516.543-n
- Garteiser P, Doblas S, Daire J-L, Wagner M, Leitao H, Vilgrain V, et al. MR elastography of liver tumours: Value of viscoelastic properties for tumour characterisation. *Eur Radiol* (2012) 22:2169–77. doi:10.1007/s00330-012-2474-6
- Bunevicius A, Schregel K, Sinkus R, Golby A, Patz S. Review: MR elastography of brain tumors. *NeuroImage: Clin* (2020) 25:102109. doi:10.1016/j.nicl.2019.102109
- Gültekin E, Wetz C, Braun J, Geisel D, Furth C, Hamm B, et al. Added value of tomoelastography for characterization of pancreatic Neuroendocrine tumor aggressiveness based on stiffness. *Cancers* (2021) 13:5185. doi:10.3390/cancers13205185
- Li J, Zormpas-Petridis K, Boulton JKR, Reeves EL, Heindl A, Vinci M, et al. Investigating the contribution of collagen to the tumor biomechanical phenotype with noninvasive magnetic resonance elastography. *Cancer Res* (2019) 79:5874–83. doi:10.1158/0008-5472.can-19-1595
- Jugé L, Doan B-T, Seguin J, Albuquerque M, Larrat B, Mignet N, et al. Colon tumor growth and Antivascular treatment in mice: Complementary assessment with MR elastography and diffusion-weighted MR imaging. *Radiology* (2012) 264:436–44. doi:10.1148/radiol.12111548
- Shahryari M, Tzschätzsch H, Guo J, Marticorena Garcia SR, Böning G, Fehrenbach U, et al. Tomoelastography distinguishes noninvasively between benign and malignant liver lesions. *Cancer Res* (2019) 79:5704–10. doi:10.1158/0008-5472.can-19-2150
- Schregel K, Nowicki MO, Palotai M, Nazari N, Zane R, Sinkus R, et al. Magnetic Resonance Elastography reveals effects of anti-angiogenic glioblastoma treatment on tumor stiffness and captures progression in an orthotopic mouse model. *Cancer Imaging* (2020) 20:35. doi:10.1186/s40644-020-00314-1
- Garteiser P, Doblas S, Van Beers BE. Magnetic resonance elastography of liver and spleen: Methods and applications. *NMR Biomed* (2018) 31:e3891. doi:10.1002/nbm.3891

Funding

This work has received funding from the European Union's Horizon 2020 research and innovation program under grant agreement N° 668039 and has been performed by a laboratory member of France Life Imaging network, supported by grant ANR-11-INBS-0006.

Conflict of interest

The authors declare that the research was conducted in the absence of any commercial or financial relationships that could be construed as a potential conflict of interest.

Publisher's note

All claims expressed in this article are solely those of the authors and do not necessarily represent those of their affiliated organizations, or those of the publisher, the editors and the reviewers. Any product that may be evaluated in this article, or claim that may be made by its manufacturer, is not guaranteed or endorsed by the publisher.

- Manduca A, Bayly PJ, Ehman RL, Kolipaka A, Royston TJ, Sack I, et al. MR elastography: Principles, guidelines, and terminology. *Magn Reson Med* (2021) 85:2377–90. doi:10.1002/mrm.28627
- Sinkus R, Lorenzen J, Schrader D, Lorenzen M, Dargatz M, Holz D. High-resolution tensor MR elastography for breast tumour detection. *Phys Med Biol* (2000) 45:1649–64. doi:10.1088/0031-9155/45/6/317
- Sahebjavaher RS, Nir G, Honarvar M, Gagnon LO, Ischia J, Jones EC, et al. MR elastography of prostate cancer: Quantitative comparison with histopathology and repeatability of methods. *NMR Biomed* (2015) 28:124–39. doi:10.1002/nbm.3218
- Litwiller DV, Mariappan YK, Ehman RL. Magnetic resonance elastography. *Curr Med Imaging Rev* (2012) 8:46–55. doi:10.2174/157340512799220562
- Reiss-Zimmermann M, Streitberger K-J, Sack I, Braun J, Arlt F, Fritsch D, et al. High resolution imaging of viscoelastic properties of intracranial tumours by multi-frequency magnetic resonance elastography. *Clin Neuroradiol* (2015) 25:371–8. doi:10.1007/s00062-014-0311-9
- Hughes JD, Fattahi N, Van Gompel J, Arani A, Ehman R, Huston J, 3rd. Magnetic resonance elastography detects tumoral consistency in pituitary macroadenomas. *Pituitary* (2016) 19:286–92. doi:10.1007/s11102-016-0706-5
- Venkatesh SK, Yin M, Glockner JF, Takahashi N, Araoz PA, Talwalkar JA, et al. MR elastography of liver tumors: Preliminary results. *Am J Roentgenology* (2008) 190:1534–40. doi:10.2214/ajr.07.3123
- Gnanago J-L, Capsal J-F, Gerges T, Lombard P, Semet V, Cottinet P-J, et al. Actuators for MRE: New perspectives with Flexible Electroactive materials. *Front Phys* (2021) 9:580. doi:10.3389/fphy.2021.633848
- Tzschätzsch H, Guo J, Dittmann F, Hirsch S, Barnhill E, Johrens K, et al. Tomoelastography by multifrequency wave number recovery from time-harmonic propagating shear waves. *Med Image Anal* (2016) 30:1–10. doi:10.1016/j.media.2016.01.001
- Dittmann F, Reiter R, Guo J, Haas M, Asbach P, Fischer T, et al. Tomoelastography of the prostate using multifrequency MR elastography and externally placed pressurized-air drivers. *Magn Reson Med* (2018) 79:1325–33. doi:10.1002/mrm.26769

20. Zhu L, Guo J, Jin Z, Xue H, Dai M, Zhang W, et al. Distinguishing pancreatic cancer and autoimmune pancreatitis with *in vivo* tomoelelastography. *Eur Radiol* (2021) 31:3366–74. doi:10.1007/s00330-020-07420-5
21. Runge JH, Hoelzl SH, Sudakova J, Dokumaci AS, Nelissen JL, Guenther C, et al. A novel magnetic resonance elastography transducer concept based on a rotational eccentric mass: Preliminary experiences with the gravitational transducer. *Phys Med Biol* (2019) 64:045007. doi:10.1088/1361-6560/aaf9f8
22. Li J, Jamin Y, Boulton JKR, Cummings C, Waterton JC, Ulloa J, et al. Tumour biomechanical response to the vascular disrupting agent ZD6126 *in vivo* assessed by magnetic resonance elastography. *Br J Cancer* (2014) 110:1727–32. doi:10.1038/bjc.2014.76
23. Jamin Y, Boulton JKR, Li J, Popov S, Garteiser P, Ulloa JL, et al. Exploring the biomechanical properties of brain Malignancies and their Pathologic determinants *in vivo* with magnetic resonance elastography. *Cancer Res* (2015) 75:1216–24. doi:10.1158/0008-5472.CAN-14-1997
24. Feng Y, Clayton EH, Okamoto RJ, Engelbach J, Bayly PV, Garbow JR. A longitudinal magnetic resonance elastography study of murine brain tumors following radiation therapy. *Phys Med Biol* (2016) 61:6121–31. doi:10.1088/0031-9155/61/16/6121
25. Sahebjavaher RS, Nir G, Gagnon LO, Ischia J, Jones EC, Chang SD, et al. MR elastography and diffusion-weighted imaging of *ex vivo* prostate cancer: Quantitative comparison to histopathology. *NMR Biomed* (2015) 28:89–100. doi:10.1002/nbm.3203
26. Pepin KM, Chen J, Glaser KJ, Mariappan YK, Reuland B, Ziesmer S, et al. MR elastography derived shear stiffness—a new imaging biomarker for the assessment of early tumor response to chemotherapy. *Magn Reson Med* (2014) 71:1834–40. doi:10.1002/mrm.24825
27. Huwart L, Salameh N, ter Beek L, Vicaut E, Peeters F, Sinkus R, et al. MR elastography of liver fibrosis: Preliminary results comparing spin-echo and echo-planar imaging. *Eur Radiol* (2008) 18:2535–41. doi:10.1007/s00330-008-1051-5
28. Shi Y, Glaser KJ, Venkatesh SK, Ben-Abraham EI, Ehman RL. Feasibility of using 3D MR elastography to determine pancreatic stiffness in healthy volunteers. *J Magn Reson Imaging* (2015) 41:369–75. doi:10.1002/jmri.24572
29. Shi Y, Xia F, Li QJ, Li JH, Yu B, Li Y, et al. Magnetic resonance elastography for the evaluation of liver fibrosis in chronic hepatitis B and C by using both gradient-Recalled echo and spin-echo echo planar imaging: A prospective study. *Am J Gastroenterol* (2016) 111:823–33. doi:10.1038/ajg.2016.56
30. Knutsson H, Westin C-F, Granlund G. Local multiscale frequency and bandwidth estimation. In: *Proceedings of 1st International Conference on Image Processing*. IEEE (1994). p. 36–40.
31. Manduca A, Muthupillai R, Rossman PJ, Greenleaf JF, Ehman RL. Local wavelength estimation for magnetic resonance elastography. In: *Proceedings of 3rd IEEE International Conference on Image Processing*. IEEE (1996). p. 527–30.
32. Kruse S, Smith J, Lawrence A, Dresner M, Manduca A, Greenleaf JF, et al. Tissue characterization using magnetic resonance elastography: Preliminary results. *Phys Med Biol* (2000) 45:1579–90. doi:10.1088/0031-9155/45/6/313
33. McKnight AL, Kugel JL, Rossman PJ, Manduca A, Hartmann LC, Ehman RL. MR elastography of breast cancer: Preliminary results. *Am J Roentgenology* (2002) 178:1411–7. doi:10.2214/ajr.178.6.1781411
34. Venkatesh SK, Yin M, Ehman RL. Magnetic resonance elastography of liver: Technique, analysis and clinical applications. *J Magn Reson Imaging* (2013) 37:544–55. doi:10.1002/jmri.24092
35. Li S, Chen M, Wang W, Zhao W, Wang J, Zhao X, et al. A feasibility study of MR elastography in the diagnosis of prostate cancer at 3.0 T. *Acta Radiol* (2011) 52:354–8. doi:10.1258/ar.2010.100276
36. Clayton EH, Okamoto RJ, Bayly PV. Mechanical properties of viscoelastic media by local frequency estimation of divergence-free wave fields. *J Biomech Eng* (2013) 135:021025. doi:10.1115/1.4023433
37. Romano AJ, Bucaro JA, Ehman R, Shirron JJ. Evaluation of a material parameter extraction algorithm using MRI-based displacement measurements. *IEEE Trans Ultrason Ferroelectr Freq Control* (2000) 47:1575–81. doi:10.1109/58.883546
38. Oliphant TE, Manduca A, Ehman RL, Greenleaf JF. Complex-valued stiffness reconstruction for magnetic resonance elastography by algebraic inversion of the differential equation. *Magn Reson Med* (2001) 45:299–310. doi:10.1002/1522-2594(200102)45:2<299::aid-mrm1039>3.0.co;2-o
39. Manduca A, Lake DS, Kruse SA, Ehman RL. Spatio-temporal directional filtering for improved inversion of MR elastography images. *Med Image Anal* (2003) 7:465–73. doi:10.1016/s1361-8415(03)00038-0
40. Sinkus R, Tanter M, Xydeas T, Catheline S, Bercoff J, Fink M. Viscoelastic shear properties of *in vivo* breast lesions measured by MR elastography. *Magn Reson Imaging* (2005) 23:159–65. doi:10.1016/j.mri.2004.11.060
41. Sinkus R, Siegmann K, Xydeas T, Tanter M, Claussen C, Fink M. MR elastography of breast lesions: Understanding the solid/liquid duality can improve the specificity of contrast-enhanced MR mammography. *Magn Reson Med* (2007) 58:1135–44. doi:10.1002/mrm.21404
42. Kwon OI, Park C, Nam HS, Woo EJ, Seo JK, Glaser KJ, et al. Shear modulus decomposition algorithm in magnetic resonance elastography. *IEEE Trans Med Imaging* (2009) 28:1526–33. doi:10.1109/tmi.2009.2019823
43. Streitberger KJ, Lilaj L, Schrank F, Braun J, Hoffmann KT, Reiss-Zimmermann M, et al. How tissue fluidity influences brain tumor progression. *Proc Natl Acad Sci U S A* (2020) 117:128–34. doi:10.1073/pnas.1913511116
44. Siegmann KC, Xydeas T, Sinkus R, Kraemer B, Vogel U, Claussen CD. Diagnostic value of MR elastography in addition to contrast-enhanced MR imaging of the breast—Initial clinical results. *Eur Radiol* (2010) 20:318–25. doi:10.1007/s00330-009-1566-4
45. Papazoglou S, Hirsch S, Braun J, Sack I. Multifrequency inversion in magnetic resonance elastography. *Phys Med Biol* (2012) 57:2329–46. doi:10.1088/0031-9155/57/8/2329
46. Hirsch S, Guo J, Reiter R, Papazoglou S, Kroencke T, Braun J, et al. MR elastography of the liver and the spleen using a piezoelectric driver, single-shot wave-field acquisition, and multifrequency dual parameter reconstruction. *Magn Reson Med* (2014) 71:267–77. doi:10.1002/mrm.24674
47. Streitberger K-J, Reiss-Zimmermann M, Freimann FB, Bayerl S, Guo J, Arlt F, et al. High-resolution mechanical imaging of glioblastoma by multifrequency magnetic resonance elastography. *PLoS one* (2014) 9:e110588. doi:10.1371/journal.pone.0110588
48. Li M, Guo J, Hu P, Jiang H, Chen J, Hu J, et al. Tomoelelastography based on multifrequency MR elastography for prostate cancer detection: Comparison with multiparametric MRI. *Radiology* (2021) 299:E259–370. doi:10.1148/radiol.2021219008
49. Honarvar M, Sahebjavaher RS, Rohling R, Salcudean SE. A comparison of finite element-based inversion algorithms, local frequency estimation, and direct inversion approach used in MRE. *IEEE Trans Med Imaging* (2017) 36:1686–98. doi:10.1109/tmi.2017.2686388
50. Honarvar M, Sahebjavaher R, Salcudean S, Rohling R. Sparsity regularization in dynamic elastography. *Phys Med Biol* (2012) 57:5909–27. doi:10.1088/0031-9155/57/19/5909
51. Van Houten EE, Paulsen KD, Miga MI, Kennedy FE, Weaver JB. An overlapping subzone technique for MR-based elastic property reconstruction. *Magn Reson Med* (1999) 42:779–86. doi:10.1002/(sici)1522-2594(199910)42:4<779::aid-mrm21>3.0.co;2-z
52. Solamen LM, McGarry MD, Tan L, Weaver JB, Paulsen KD. Phantom evaluations of nonlinear inversion MR elastography. *Phys Med Biol* (2018) 63:145021. doi:10.1088/1361-6560/aac08
53. Honarvar M, Rohling R, Salcudean SE. A comparison of direct and iterative finite element inversion techniques in dynamic elastography. *Phys Med Biol* (2016) 61:3026–48. doi:10.1088/0031-9155/61/8/3026
54. Loomba R, Cui J, Wolfson T, Haufe W, Hooker J, Szevenyi N, et al. Novel 3D magnetic resonance elastography for the noninvasive diagnosis of advanced fibrosis in NAFLD: A prospective study. *Am J Gastroenterol* (2016) 111:986–94. doi:10.1038/ajg.2016.65
55. Morisaka H, Motosugi U, Glaser KJ, Ichikawa S, Ehman RL, Sano K, et al. Comparison of diagnostic accuracies of two- and three-dimensional MR elastography of the liver. *J Magn Reson Imaging* (2017) 45:1163–70. doi:10.1002/jmri.25425
56. Wagner M, Besa C, Bou Ayache J, Yasar TK, Bane O, Fung M, et al. Magnetic resonance elastography of the liver: Qualitative and quantitative comparison of gradient echo and spin echo Echoplanar imaging sequences. *Invest Radiol* (2016) 51:575–81. doi:10.1097/rli.0000000000000269
57. Svensson SF, De Arcos J, Darwish OI, Fraser-Green J, Storås TH, Holm S, et al. Robustness of MR elastography in the healthy brain: Repeatability, reliability, and effect of different reconstruction methods. *J Magn Reson Imaging* (2021) 53:1510–21. doi:10.1002/jmri.27475
58. Fovargue D, Kozerke S, Sinkus R, Nordsletten D. Robust MR elastography stiffness quantification using a localized divergence free finite element reconstruction. *Med Image Anal* (2018) 44:126–42. doi:10.1016/j.media.2017.12.005
59. Shi Y, Gao F, Li Y, Tao S, Yu B, Liu Z, et al. Differentiation of benign and malignant solid pancreatic masses using magnetic resonance elastography with spin-echo echo planar imaging and three-dimensional inversion reconstruction: A prospective study. *Eur Radiol* (2018) 28:936–45. doi:10.1007/s00330-017-5062-y

60. Bilton LE. Soft tissue rheology and its implications for elastography: Challenges and opportunities. *NMR Biomed* (2018) 31:e3832. doi:10.1002/nbm.3832
61. Asbach P, Klatt D, Schlosser B, Biermer M, Mueche M, Rieger A, et al. Viscoelasticity-based staging of hepatic fibrosis with multifrequency MR elastography. *Radiology* (2010) 257:80–6. doi:10.1148/radiol.10092489
62. Sack I, Jöhrens K, Würfel J, Braun J. Structure-sensitive elastography: On the viscoelastic powerlaw behavior of *in vivo* human tissue in health and disease. *Soft Matter* (2013) 9:5672–80. doi:10.1039/c3sm50552a
63. Garteiser P, Pagé G, d'Assignies G, Leita HS, Vilgrain V, Sinkus R, et al. Necro-inflammatory activity grading in chronic viral hepatitis with three-dimensional multifrequency MR elastography. *Sci Rep* (2021) 11:19386. doi:10.1038/s41598-021-98726-x
64. Gennisson JL, Defieux T, Fink M, Tanter M. Ultrasound elastography: Principles and techniques. *Diagn Interv Imaging* (2013) 94:487–95. doi:10.1016/j.diii.2013.01.022
65. Barr RG. Liver elastography still in its Infancy. *Radiology* (2018) 288:107–8. doi:10.1148/radiol.2018180777
66. Lu P, Weaver VM, Werb Z. The extracellular matrix: A dynamic niche in cancer progression. *J Cell Biol* (2012) 196:395–406. doi:10.1083/jcb.2011102147
67. Hanahan D, Coussens LM. Accessories to the crime: Functions of cells recruited to the tumor microenvironment. *Cancer cell* (2012) 21:309–22. doi:10.1016/j.ccr.2012.02.022
68. Jain RK. Normalizing tumor microenvironment to treat cancer: Bench to bedside to biomarkers. *Am J Clin Oncol* (2013) 31:2205–18. doi:10.1200/jco.2012.46.3653
69. Correia AL, Bissell MJ. The tumor microenvironment is a dominant force in multidrug resistance. *Drug Resist updates* (2012) 15:39–49. doi:10.1016/j.drug.2012.01.006
70. Jain RK, Martin JD, Stylianopoulos T. The role of mechanical forces in tumor growth and therapy. *Annu Rev Biomed Eng* (2014) 16:321–46. doi:10.1146/annurev-bioeng-071813-105259
71. Kalli M, Papageorgis P, Gkretsi V, Stylianopoulos T. Solid stress facilitates fibroblasts activation to promote pancreatic cancer cell migration. *Ann Biomed Eng* (2018) 46:657–69. doi:10.1007/s10439-018-1997-7
72. Rahbari NN, Kedrin D, Incio J, Liu H, Ho WW, Nia HT, et al. Anti-VEGF therapy induces ECM remodeling and mechanical barriers to therapy in colorectal cancer liver metastases. *Sci Transl Med* (2016) 8:360ra135. doi:10.1126/scitranslmed.aaf5219
73. Riegler J, Labyed Y, Rosenzweig S, Savinal V, Castiglioni A, Dominguez CX, et al. Tumor elastography and its association with collagen and the tumor microenvironment. *Clin Cancer Res* (2018) 24:4455–67. doi:10.1158/1078-0432.CCR-17-3262
74. Mitchell MJ, Jain RK, Langer R. Engineering and physical sciences in oncology: Challenges and opportunities. *Nat Rev Cancer* (2017) 17:659–75. doi:10.1038/nrc.2017.83
75. Park SJ, Yoon JH, Lee DH, Lim WH, Lee JM. Tumor stiffness measurements on MR elastography for single Nodular hepatocellular carcinomas can predict tumor recurrence after hepatic resection. *J Magn Reson Imaging* (2021) 53:587–96. doi:10.1002/jmri.27359
76. Salameh N, Larrat B, Abarca-Quinones J, Pallu S, Dorvillius M, Leclercq I, et al. Early detection of steatohepatitis in fatty rat liver by using MR elastography. *Radiology* (2009) 253:90–7. doi:10.1148/radiol.2523081817
77. Ronot M, Lambert S, Elkrief L, Doblus S, Rautou P-E, Castera L, et al. Assessment of portal hypertension and high-risk oesophageal varices with liver and spleen three-dimensional multifrequency MR elastography in liver cirrhosis. *Eur Radiol* (2014) 24:1394–402. doi:10.1007/s00330-014-3124-y
78. Nia HT, Liu H, Seano G, Datta M, Jones D, Rahbari N, et al. Solid stress and elastic energy as measures of tumour mechanopathology. *Nat Biomed Eng* (2017) 1:0004. doi:10.1038/s41551-016-0004
79. Stylianopoulos T, Munn LL, Jain RK. Reengineering the physical microenvironment of tumors to improve drug delivery and efficacy: From mathematical modeling to bench to bedside. *Trends Cancer* (2018) 4:292–319. doi:10.1016/j.trecan.2018.02.005
80. Nieskoski MD, Marra K, Gunn JR, Kanick SC, Doyle MM, Hasan T, et al. Separation of solid stress from interstitial fluid pressure in pancreas cancer correlates with collagen area fraction. *J Biomech Eng* (2017) 139. doi:10.1115/1.4036392
81. Broders-Bondon F, Nguyen Ho-Bouldoires TH, Fernandez-Sanchez ME, Farge E. Mechanotransduction in tumor progression: The dark side of the force. *J Cell Biol* (2018) 217:1571–87. doi:10.1083/jcb.201701039
82. Nguyen Ho-Bouldoires TH, Sollier K, Zamfirov L, Broders-Bondon F, Mitrossilis D, Bermeo S, et al. Ret kinase-mediated mechanical induction of colon stem cells by tumor growth pressure stimulates cancer progression *in vivo*. *Commun Biol* (2022) 5:137. doi:10.1038/s42003-022-03079-4
83. Fernández-Sánchez ME, Barbier S, Whitehead J, Béalle G, Michel A, Latorre-Ossa H, et al. Mechanical induction of the tumorigenic β -catenin pathway by tumour growth pressure. *Nature* (2015) 523:92–5. doi:10.1038/nature14329
84. Mierke CT. The matrix environmental and cell mechanical properties regulate cell migration and contribute to the invasive phenotype of cancer cells. *Rep Prog Phys* (2019) 82:064602. doi:10.1088/1361-6633/ab1628
85. Huang Y, Goel S, Duda DG, Fukumura D, Jain RK. Vascular normalization as an emerging strategy to enhance cancer immunotherapy. *Cancer Res* (2013) 73:2943–8. doi:10.1158/0008-5472.can-12-4354
86. Pries AR, Höpfner M, le Noble F, Dewhirst MW, Secomb TW. The shunt problem: Control of functional shunting in normal and tumour vasculature. *Nat Rev Cancer* (2010) 10:587–93. doi:10.1038/nrc2895
87. Wilson WR, Hay MP. Targeting hypoxia in cancer therapy. *Nat Rev Cancer* (2011) 11:393–410. doi:10.1038/nrc3064
88. Boucher Y, Kirkwood JM, Opacic D, Desantis M, Jain RK. Interstitial hypertension in superficial metastatic melanomas in humans. *Cancer Res* (1991) 51:6691–4.
89. Jain RK, Tong RT, Munn LL. Effect of vascular normalization by antiangiogenic therapy on interstitial hypertension, peritumor edema, and lymphatic metastasis: Insights from a mathematical model. *Cancer Res* (2007) 67:2729–35. doi:10.1158/0008-5472.can-06-4102
90. Melo V, Bremer E, Martin JD. Towards immunotherapy-induced normalization of the tumor microenvironment. *Front Cell Dev Biol* (2022) 10:908389. doi:10.3389/fcell.2022.908389
91. Hidalgo M. Pancreatic cancer. *N Engl J Med Overseas Ed* (2010) 362:1605–17. doi:10.1056/nejmra0901557
92. Laklai H, Miroshnikova YA, Pickup MW, Collisson EA, Kim GE, Barrett AS, et al. Genotype tunes pancreatic ductal adenocarcinoma tissue tension to induce matricellular fibrosis and tumor progression. *Nat Med* (2016) 22:497–505. doi:10.1038/nm.4082
93. Neschadim A, Summerlee AJ, Silvertown JD. Targeting the relaxin hormonal pathway in prostate cancer. *Int J Cancer* (2015) 137:2287–95. doi:10.1002/ijc.29079
94. Atkinson JM, Falconer RA, Edwards DR, Pennington CJ, Siller CS, Shnyder SD, et al. Development of a novel tumor-targeted vascular disrupting agent activated by membrane-type matrix metalloproteinases. *Cancer Res* (2010) 70:6902–12. doi:10.1158/0008-5472.can-10-1440
95. Provenzano PP, Cuevas C, Chang AE, Goel VK, Von Hoff DD, Hingorani SR. Enzymatic targeting of the stroma ablates physical barriers to treatment of pancreatic ductal adenocarcinoma. *Cancer Cell* (2012) 21:418–29. doi:10.1016/j.ccr.2012.01.007
96. Chauhan VP, Martin JD, Liu H, Lacorre DA, Jain SR, Kozin SV, et al. Angiotensin inhibition enhances drug delivery and potentiates chemotherapy by decompressing tumour blood vessels. *Nat Commun* (2013) 4:2516. doi:10.1038/ncomms3516
97. Murphy JE, Wo JY, Ryan DP, Clark JW, Jiang W, Yeap BY, et al. Total Neoadjuvant therapy with FOLFIRINOX in combination with losartan followed by Chemoradiotherapy for locally advanced pancreatic cancer: A phase 2 clinical trial. *JAMA Oncol* (2019) 5:1020–7. doi:10.1001/jamaoncol.2019.0892
98. Van Cutsem E, Danielewicz I, Saunders MP, Pfeiffer P, Argilés G, Borg C, et al. Trifluridine/tipiracil plus bevacizumab in patients with untreated metastatic colorectal cancer ineligible for intensive therapy: The randomized TASCO1 study. *Ann Oncol* (2020) 31:1160–8. doi:10.1016/j.annonc.2020.05.024
99. Piersma B, Hayward MK, Weaver VM. Fibrosis and cancer: A strained relationship. *Biochim Biophys Acta - Rev Cancer* (2020) 1873:188356. doi:10.1016/j.bbcan.2020.188356
100. Ulrich TA, Pardo EMdJ, Kumar S. The mechanical rigidity of the extracellular matrix Regulates the structure, Motility, and proliferation of glioma cells. *Cancer Res* (2009) 69:4167–74. doi:10.1158/0008-5472.can-08-4859
101. Weigelin B, Bakker GJ, Friedl P. Intravital third harmonic generation microscopy of collective melanoma cell invasion: Principles of interface guidance and microvesicle dynamics. *Intravital* (2012) 1:32–43. doi:10.4161/intv.21223
102. Blehm BH, Jiang N, Kotobuki Y, Tanner K. Deconstructing the role of the ECM microenvironment on drug efficacy targeting MAPK signaling in a pre-clinical platform for cutaneous melanoma. *Biomaterials* (2015) 56:129–39. doi:10.1016/j.biomaterials.2015.03.041
103. Bhattacherjee S, Hamberger F, Ravichandra A, Miller M, Nair A, Affo S, et al. Tumor restriction by type I collagen opposes tumor-promoting effects of cancer-associated fibroblasts. *J Clin Invest* (2021) 131:146987. doi:10.1172/jci146987

104. Wu PH, Aroush DR, Asnacios A, Chen WC, Dokukin ME, Doss BL, et al. A comparison of methods to assess cell mechanical properties. *Nat Methods* (2018) 15: 491–8. doi:10.1038/s41592-018-0015-1
105. Kennedy P, Wagner M, Castéra L, Hong CW, Johnson CL, Sirlin CB, et al. Quantitative elastography methods in liver disease: Current Evidence and future directions. *Radiology* (2018) 286:738–63. doi:10.1148/radiol.2018170601
106. Stylianopoulos T, Martin JD, Chauhan VP, Jain SR, Diop-Frimpong B, Bardeesy N, et al. Causes, consequences, and remedies for growth-induced solid stress in murine and human tumors. *Proc Natl Acad Sci U S A* (2012) 109:15101–8. doi:10.1073/pnas.1213353109
107. Sarntinoranont M, Rooney F, Ferrari M. Interstitial stress and fluid pressure within a growing tumor. *Ann Biomed Eng* (2003) 31:327–35. doi:10.1114/1.1554923
108. Islam MT, Righetti R. A new poroelastography method to assess the solid stress distribution in cancers. *IEEE Access* (2019) 7:103404–15. doi:10.1109/access.2019.2929021
109. Islam MT, Tasciotti E, Righetti R. Non-invasive imaging of normalized solid stress in cancers *in vivo*. *IEEE J Transl Eng Health Med* (2019) 7:1–9. doi:10.1109/jtehm.2019.2932059
110. Fovargue D, Fiorito M, Capilnasiu A, Nordsletten D, Lee J, Sinkus R. Towards noninvasive estimation of tumour pressure by utilising MR elastography and nonlinear biomechanical models: A simulation and phantom study. *Sci Rep* (2020) 10:5588–13. doi:10.1038/s41598-020-62367-3
111. Nia HT, Munn LL, Jain RK. Mapping physical tumor microenvironment and drug delivery. *Clin Cancer Res* (2019) 25:2024–6. doi:10.1158/1078-0432.ccr-18-3724
112. Clarke EC, Cheng S, Green M, Sinkus R, Bilston LE. Using static preload with magnetic resonance elastography to estimate large strain viscoelastic properties of bovine liver. *J Biomech* (2011) 44:2461–5. doi:10.1016/j.jbiomech.2011.06.023
113. Page G, Tardieu M, Besret L, Blot L, Lopes J, Sinkus R, et al. Assessing tumor mechanics by MR elastography at different strain levels. *J Magn Reson Imaging* (2019) 50:1982–9. doi:10.1002/jmri.26787
114. Pagé G, Tardieu M, Gennisson JL, Besret L, Garteiser P, Van Beers BE. Tumor solid stress: Assessment with MR elastography under compression of patient-derived hepatocellular carcinomas and cholangiocarcinomas xenografted in mice. *Cancers* (2021) 13:1891. doi:10.3390/cancers13081891
115. Rotemberg V, Palmeri M, Nightingale R, Rouze N, Nightingale K. The impact of hepatic pressurization on liver shear wave speed estimates in constrained versus unconstrained conditions. *Phys Med Biol* (2012) 57:329–41. doi:10.1088/0031-9155/57/2/329
116. Gennisson J-L, Grenier N, Combe C, Tanter M. Supersonic shear wave elastography of *in vivo* pig kidney: Influence of blood pressure, urinary pressure and tissue anisotropy. *Ultrasound Med Biol* (2012) 38:1559–67. doi:10.1016/j.ultrasmedbio.2012.04.013
117. Talwalkar JA, Yin M, Venkatesh S, Rossman PJ, Grimm RC, Manduca A, et al. Feasibility of *in vivo* MR elastographic splenic stiffness measurements in the assessment of portal hypertension. *Am J Roentgenology* (2009) 193:122–7. doi:10.2214/ajr.07.3504
118. Morisaka H, Motosugi U, Ichikawa T, Sano K, Ichikawa S, Araki T, et al. MR-based measurements of portal vein flow and liver stiffness for predicting gastroesophageal varices. *Magn Reson Med Sci* (2013) 12:77–86. doi:10.2463/mrms.2012-0052
119. Huang SY, Abdelsalam ME, Harmoush S, Ensor JE, Chetta JA, Hwang K-P, et al. Evaluation of liver fibrosis and hepatic venous pressure gradient with MR elastography in a novel swine model of cirrhosis. *J Magn Reson Imaging* (2014) 39: 590–7. doi:10.1002/jmri.24189
120. Hompland T, Ellingsen C, Øvrebø KM, Rofstad EK. Interstitial fluid pressure and associated lymph node metastasis revealed in tumors by dynamic contrast-enhanced MRI. *Cancer Res* (2012) 72:4899–908. doi:10.1158/0008-5472.can-12-0903
121. Elmghirbi R, Nagaraja TN, Brown SL, Keenan KA, Panda S, Cabral G, et al. Toward a noninvasive estimate of interstitial fluid pressure by dynamic contrast-enhanced MRI in a rat model of cerebral tumor. *Magn Reson Med* (2018) 80: 2040–52. doi:10.1002/mrm.27163
122. Ahmed R, Ye J, Gerber SA, Linehan DC, Doyley MM. Preclinical imaging using single Track location shear wave elastography: Monitoring the progression of murine pancreatic tumor liver metastasis *in vivo*. *IEEE Trans Med Imaging* (2020) 39:2426–39. doi:10.1109/tmi.2020.2971422
123. Wang H, Mills B, Mislati R, Ahmed R, Gerber SA, Linehan D, et al. Shear wave elastography can differentiate between radiation-responsive and non-responsive pancreatic tumors: An *ex vivo* study with murine models. *Ultrasound Med Biol* (2020) 46:393–404. doi:10.1016/j.ultrasmedbio.2019.10.005
124. Wang H, Mislati R, Ahmed R, Vincent P, Nwabunwanne SF, Gunn JR, et al. Elastography can map the local inverse relationship between shear modulus and drug delivery within the pancreatic ductal adenocarcinoma microenvironment. *Clin Cancer Res* (2019) 25:2136–43. doi:10.1158/1078-0432.ccr-18-2684
125. Vincent P, Wang H, Nieskoski M, Gunn JR, Marra K, Hoopes PJ, et al. High-resolution *ex vivo* elastography to characterize tumor stromal heterogeneity *in Situ* in pancreatic adenocarcinoma. *IEEE Trans Biomed Eng* (2020) 67:2490–6. doi:10.1109/tbme.2019.2963562
126. Huwart L, Sempoux C, Vicaut E, Salameh N, Annet L, Danse E, et al. Magnetic resonance elastography for the noninvasive staging of liver fibrosis. *Gastroenterology* (2008) 135:32–40. doi:10.1053/j.gastro.2008.03.076
127. Kim D, Kim WR, Talwalkar JA, Kim HJ, Ehman RL. Advanced fibrosis in nonalcoholic fatty liver disease: Noninvasive assessment with MR elastography. *Radiology* (2013) 268:411–9. doi:10.1148/radiol.13121193
128. Looma R, Wolfson T, Ang B, Hooker J, Behling C, Peterson M, et al. Magnetic resonance elastography predicts advanced fibrosis in patients with nonalcoholic fatty liver disease: A prospective study. *Hepatology* (2014) 60: 1920–8. doi:10.1002/hep.27362
129. Ichikawa S, Motosugi U, Nakazawa T, Morisaka H, Sano K, Ichikawa T, et al. Hepatitis activity should be considered a confounder of liver stiffness measured with MR elastography. *J Magn Reson Imaging* (2015) 41:1203–8. doi:10.1002/jmri.24666
130. Yin M, Glaser KJ, Talwalkar JA, Chen J, Manduca A, Ehman RL. Hepatic MR elastography: Clinical performance in a series of 1377 Consecutive examinations. *Radiology* (2016) 278:114–24. doi:10.1148/radiol.2015142141
131. Imajo K, Kessoku T, Honda Y, Tomono W, Ogawa Y, Mawatari H, et al. Magnetic resonance imaging more accurately Classifies Steatosis and fibrosis in patients with nonalcoholic fatty liver disease than transient elastography. *Gastroenterology* (2016) 150:626–37.e7. doi:10.1053/j.gastro.2015.11.048
132. Ichikawa S, Motosugi U, Enomoto N, Matsuda M, Onishi H. Noninvasive hepatic fibrosis staging using MR elastography: The usefulness of the bayesian prediction method. *J Magn Reson Imaging* (2017) 46:375–82. doi:10.1002/jmri.25551
133. Gharib AM, Han MAT, Meissner EG, Kleiner DE, Zhao X, McLaughlin M, et al. Magnetic resonance elastography shear wave velocity correlates with liver fibrosis and hepatic venous pressure gradient in Adults with advanced liver disease. *Biomed Research International* (2017) 2017:1–8. doi:10.1155/2017/2067479
134. Forner A, Reig M, Bruix J. Hepatocellular carcinoma. *The Lancet* (2018) 391: 1301–14. doi:10.1016/s0140-6736(18)30010-2
135. Motosugi U, Ichikawa T, Koshiishi T, Sano K, Morisaka H, Ichikawa S, et al. Liver stiffness measured by magnetic resonance elastography as a risk factor for hepatocellular carcinoma: A preliminary case-control study. *Eur Radiol* (2013) 23: 156–62. doi:10.1007/s00330-012-2571-6
136. Ichikawa S, Motosugi U, Enomoto N, Onishi H. Magnetic resonance elastography can predict development of hepatocellular carcinoma with longitudinally acquired two-point data. *Eur Radiol* (2019) 29:1013–21. doi:10.1007/s00330-018-5640-7
137. Van Beers BE, Daire JL, Garteiser P. New imaging techniques for liver diseases. *J Hepatol* (2015) 62:690–700. doi:10.1016/j.jhep.2014.10.014
138. Hennedige TP, Hallinan JT, Leung FP, Teo LL, Iyer S, Wang G, et al. Comparison of magnetic resonance elastography and diffusion-weighted imaging for differentiating benign and malignant liver lesions. *Eur Radiol* (2016) 26: 398–406. doi:10.1007/s00330-015-3835-8
139. Marasco G, Colecchia A, Colli A, Ravaioli F, Casazza G, Bacchi Reggiani ML, et al. Role of liver and spleen stiffness in predicting the recurrence of hepatocellular carcinoma after resection. *J Hepatol* (2019) 70:440–8. doi:10.1016/j.jhep.2018.10.022
140. Kairaluoma V, Kemi N, Pohjanen VM, Saarnio J, Helminen O. Tumour budding and tumour-stroma ratio in hepatocellular carcinoma. *Br J Cancer* (2020) 123:38–45. doi:10.1038/s41416-020-0847-1
141. Wang J, Shan Q, Liu Y, Yang H, Kuang S, He B, et al. 3D MR elastography of hepatocellular carcinomas as a potential biomarker for predicting tumor recurrence. *J Magn Reson Imaging* (2019) 49:719–30. doi:10.1002/jmri.26250
142. Cho HJ, Kim B, Kim HJ, Huh J, Kim JK, Lee JH, et al. Liver stiffness measured by MR elastography is a predictor of early HCC recurrence after treatment. *Eur Radiol* (2020) 30:4182–92. doi:10.1007/s00330-020-06792-y
143. Gordic S, Ayache JB, Kennedy P, Besa C, Wagner M, Bane O, et al. Value of tumor stiffness measured with MR elastography for assessment of response of hepatocellular carcinoma to locoregional therapy. *Abdom Radiol (Ny)* (2017) 42: 1685–94. doi:10.1007/s00261-017-1066-y
144. Qayyum A, Hwang KP, Stafford J, Verma A, Maru DM, Sandesh S, et al. Immunotherapy response evaluation with magnetic resonance elastography (MRE) in advanced HCC. *J Immunother Cancer* (2019) 7:329. doi:10.1186/s40425-019-0766-y
145. Barton MB, Harris R, Fletcher SW. Does this patient have breast cancer?: The screening clinical breast examination: Should it be done? How? *Jama* (1999) 282: 1270–80. doi:10.1001/jama.282.13.1270

146. Mann RM, Cho N, Moy L. Breast MRI: State of the Art. *Radiology* (2019) 292: 520–36. doi:10.1148/radiol.2019182947
147. Saadatmand S, Geuzing HA, Rutgers EJT, Mann RM, de Roy van Zuidewijn DBW, Zonderland HM, et al. MRI versus mammography for breast cancer screening in women with familial risk (FaMRIS): A multicentre, randomised, controlled trial. *Lancet Oncol* (2019) 20:1136–47. doi:10.1016/s1470-2045(19)30275-x
148. Lorenzen J, Sinkus R, Lorenzen M, Dargatz M, Leussler C, Röschmann P, et al. MR elastography of the breast: preliminary clinical results. *Rofo Fortschr Geb Rontgenstr Neuen Bildgeb Verfahr* (2002) 174:830–4. doi:10.1055/s-2002-32690
149. Sinkus R, Tanter M, Catheline S, Lorenzen J, Kuhl C, Sondermann E, et al. Imaging anisotropic and viscous properties of breast tissue by magnetic resonance-elastography. *Magn Reson Med* (2005) 53:372–87. doi:10.1002/mrm.20355
150. Xydeas T, Siegmund K, Sinkus R, Krainick-Strobel U, Miller S, Claussen CD. Magnetic resonance elastography of the breast: Correlation of signal intensity data with viscoelastic properties. *Invest Radiol* (2005) 40:412–20. doi:10.1097/01.rli.0000166940.72971.4a
151. Balleyguier C, Lakhdar AB, Dunant A, Mathieu MC, Delaloge S, Sinkus R. Value of whole breast magnetic resonance elastography added to MRI for lesion characterization. *NMR Biomed* (2018) 31:e3795. doi:10.1002/nbm.3795
152. Itoh A, Ueno E, Tohno E, Kamma H, Takahashi H, Shiina T, et al. Breast disease: Clinical application of US elastography for diagnosis. *Radiology* (2006) 239: 341–50. doi:10.1148/radiol.2391041676
153. Schwab F, Redling K, Siebert M, Schötzau A, Schoenenberger CA, Zanetti-Dällenbach R. Inter- and Intra-Observer agreement in ultrasound BI-RADS classification and real-time elastography Tsukuba score assessment of breast lesions. *Ultrasound Med Biol* (2016) 42:2622–9. doi:10.1016/j.ultrasmedbio.2016.06.017
154. Murphy MC, Huston J, 3rd, Glaser KJ, Manduca A, Meyer FB, Lanzino G, et al. Preoperative assessment of meningioma stiffness using magnetic resonance elastography. *J Neurosurg* (2013) 118:643–8. doi:10.3171/2012.9.jns.12519
155. Hughes JD, Fattahi N, Van Gompel J, Arani A, Meyer F, Lanzino G, et al. Higher-resolution magnetic resonance elastography in meningiomas to determine Intratumoral consistency. *Neurosurgery* (2015) 77:653–9. discussion 658–9. doi:10.1227/neu.0000000000000892
156. Sakai N, Takehara Y, Yamashita S, Ohishi N, Kawaji H, Sameshima T, et al. Shear stiffness of 4 common intracranial tumors measured using MR elastography: Comparison with Intraoperative consistency grading. *AJNR Am J Neuroradiol* (2016) 37:1851–9. doi:10.3174/ajnr.a4832
157. Arani A, Manduca A, Ehman RL, Huston J, Iii. Harnessing brain waves: A review of brain magnetic resonance elastography for clinicians and scientists entering the field. *Br J Radiol* (2021) 94:20200265. doi:10.1259/bjr.20200265
158. Yin Z, Lu X, Cohen Cohen S, Sui Y, Manduca A, Van Gompel JJ, et al. A new method for quantification and 3D visualization of brain tumor adhesion using slip interface imaging in patients with meningiomas. *Eur Radiol* (2021) 31:5554–64. doi:10.1007/s00330-021-07918-6
159. Simon M, Guo J, Papazoglou S, Scholand-Engler H, Erdmann C, Melchert U, et al. Non-invasive characterization of intracranial tumors by magnetic resonance elastography. *New J Phys* (2013) 15:085024. doi:10.1088/1367-2630/15/8/085024
160. Miroshnikova YA, Mouw JK, Barnes JM, Pickup MW, Lakin JN, Kim Y, et al. Tissue mechanics promote IDH1-dependent HIF1 α -tenascin C feedback to regulate glioblastoma aggression. *Nat Cell Biol* (2016) 18:1336–45. doi:10.1038/ncb3429
161. Pepin KM, McGee KP, Arani A, Lake DS, Glaser KJ, Manduca A, et al. MR elastography analysis of glioma stiffness and IDH1-mutation status. *AJNR Am J Neuroradiol* (2018) 39:31–6. doi:10.3174/ajnr.a5415
162. Murphy MC, Huston J, 3rd, Ehman RL. MR elastography of the brain and its application in neurological diseases. *Neuroimage* (2019) 187:176–83. doi:10.1016/j.neuroimage.2017.10.008
163. Romano A, Scheel M, Hirsch S, Braun J, Sack I. *In vivo* waveguide elastography of white matter tracts in the human brain. *Magn Reson Med* (2012) 68:1410–22. doi:10.1002/mrm.24141
164. Tweten DJ, Okamoto RJ, Bayly PV. Requirements for accurate estimation of anisotropic material parameters by magnetic resonance elastography: A computational study. *Magn Reson Med* (2017) 78:2360–72. doi:10.1002/mrm.26600
165. Babaei B, Fovargue D, Lloyd RA, Miller R, Jugé L, Kaplan M, et al. Magnetic resonance elastography reconstruction for anisotropic tissues. *Med Image Anal* (2021) 74:102212. doi:10.1016/j.media.2021.102212
166. Ahmed HU, El-Shater Bosaily A, Brown LC, Gabe R, Kaplan R, Parmar MK, et al. Diagnostic accuracy of multi-parametric MRI and TRUS biopsy in prostate cancer (PROMIS): A paired validating confirmatory study. *The Lancet* (2017) 389: 815–22. doi:10.1016/s0140-6736(16)32401-1
167. Tuxhorn JA, Ayala GE, Rowley DR. Reactive stroma in prostate cancer progression. *J Urol* (2001) 166:2472–83. doi:10.1016/s0022-5347(05) 65620-0
168. Burns-Cox N, Avery NC, Gingell JC, Bailey AJ. Changes in collagen metabolism in prostate cancer: A host response that may alter progression. *J Urol* (2001) 166:1698–701. doi:10.1016/s0022-5347(05)65656-x
169. Arani A, Plewes D, Chopra R. Transurethral prostate magnetic resonance elastography: Prospective imaging requirements. *Magn Reson Med* (2011) 65: 340–9. doi:10.1002/mrm.22633
170. Arani A, Plewes D, Krieger A, Chopra R. The feasibility of endorectal MR elastography for prostate cancer localization. *Magn Reson Med* (2011) 66:1649–57. doi:10.1002/mrm.22967
171. Li D, Xie K, Wolff R, Abbruzzese JL. Pancreatic cancer. *The Lancet* (2004) 363:1049–57. doi:10.1016/s0140-6736(04)15841-8
172. Eibl G, Cruz-Monserrate Z, Korc M, Petrov MS, Goodarzi MO, Fisher WE, et al. Diabetes Mellitus and Obesity as risk factors for pancreatic cancer. *J Acad Nutr Diet* (2018) 118:555–67. doi:10.1016/j.jand.2017.07.005
173. Dittmann F, Tzschätzsch H, Hirsch S, Barnhill E, Braun J, Sack I, et al. Tomoelastography of the abdomen: Tissue mechanical properties of the liver, spleen, kidney, and pancreas from single MR elastography scans at different hydration states. *Magn Reson Med* (2017) 78:976–83. doi:10.1002/mrm.26484
174. Serai SD, Abu-El-Haija M, Trout AT. 3D MR elastography of the pancreas in children. *Abdom Radiol* (2019) 44:1834–40. doi:10.1007/s00261-019-01903-w
175. Steinkohl E, Bertoli D, Hansen TM, Olesen SS, Drewes AM, Frøkjær JB. Practical and clinical applications of pancreatic magnetic resonance elastography: A systematic review. *Abdom Radiol* (2021) 46:4744–47. doi:10.1007/s00261-021-03143-3
176. Lee CU, Glockner JF, Glaser KJ, Yin M, Chen J, Kawashima A, et al. MR elastography in renal transplant patients and correlation with renal allograft biopsy: A feasibility study. *Acad Radiol* (2012) 19:834–41. doi:10.1016/j.acra.2012.03.003
177. Marticorena Garcia SR, Grossmann M, Lang ST, Tzschätzsch H, Dittmann F, Hamm B, et al. Tomoelastography of the native kidney: Regional variation and physiological effects on *in vivo* renal stiffness. *Magn Reson Med* (2018) 79:2126–34. doi:10.1002/mrm.26892
178. Prezzi D, Neji R, Kelly-Morland C, Verma H, O'Brien T, Challacombe B, et al. Characterization of small renal tumors with magnetic resonance elastography: A feasibility study. *Invest Radiol* (2018) 53:344–51. doi:10.1097/rli.0000000000000449
179. Göya C, Daggulli M, Hamidi C, Yavuz A, Hattapoglu S, Cetincakmak MG, et al. The role of quantitative measurement by acoustic radiation force impulse imaging in differentiating benign renal lesions from malignant renal tumours. *Radiol Med* (2015) 120:296–303. doi:10.1007/s11547-014-0443-7
180. Kumada T, Toyoda H, Yasuda S, Sone Y, Ogawa S, Takeshima K, et al. Prediction of hepatocellular carcinoma by liver stiffness measurements using magnetic resonance elastography after Eradicating hepatitis C Virus. *Clin Transl Gastroenterol* (2021) 12:e00337. doi:10.14309/ctg.0000000000000337
181. Zorgani A, Souchon R, Dinh AH, Chapelon JY, Ménager JM, Lounis S, et al. Brain palpation from physiological vibrations using MRI. *Proc Natl Acad Sci U S A* (2015) 112:12917–21. doi:10.1073/pnas.1509895112
182. Bohte A, Nelissen J, Runge J, Holub O, Lambert S, de Graaf L, et al. Breast magnetic resonance elastography: A review of clinical work and future perspectives. *NMR Biomed* (2018) 31:e3932. doi:10.1002/nbm.3932
183. Bertalan G, Guo J, Tzschätzsch H, Klein C, Barnhill E, Sack I, et al. Fast tomoeelastography of the mouse brain by multifrequency single-shot MR elastography. *Magn Reson Med* (2019) 81:2676–87. doi:10.1002/mrm.27586
184. Bertalan G, Klein C, Schreyer S, Steiner B, Kreft B, Tzschätzsch H, et al. Biomechanical properties of the hypoxic and dying brain quantified by magnetic resonance elastography. *Acta Biomater* (2020) 101:395–402. doi:10.1016/j.actbio.2019.11.011
185. Barnhill E, Davies PJ, Ariyurek C, Fehlnar A, Braun J, Sack I. Heterogeneous Multifrequency Direct Inversion (HMDI) for magnetic resonance elastography with application to a clinical brain exam. *Med Image Anal* (2018) 46:180–8. doi:10.1016/j.media.2018.03.003
186. Perepelyuk M, Chin L, Cao X, Oosten Av., Shenoy VB, Janmey PA, et al. Normal and fibrotic rat livers demonstrate shear strain softening and compression stiffening: A model for soft tissue mechanics. *PLOS ONE* (2016) 11:e0146588. doi:10.1371/journal.pone.0146588
187. van Oosten ASG, Chen X, Chin L, Cruz K, Patteson AE, Pogoda K, et al. Emergence of tissue-like mechanics from fibrous networks confined by close-packed cells. *Nature* (2019) 573:96–101. doi:10.1038/s41586-019-1516-5
188. Page G, Garteiser P, Paradis V, Sinkus R, Vilgrain V, Van Beers BE. *Microvascular invasion in patients with hepatocellular carcinoma: Assessment with compression MR elastography*. London (United Kingdom): Proceedings of ISMRM (2022).
189. Hu X, Zhou J, Li Y, Wang Y, Guo J, Sack I, et al. Added value of viscoelasticity for MRI-based prediction of Ki-67 expression of hepatocellular carcinoma using a deep learning combined radiomics (DLCR) model. *Cancers* (2022) 14:2575. doi:10.3390/cancers14112575